

Multiscale Simulation of Surface Defect Influence in Nanoindentation by the Quasi-Continuum Method [†]

Zhongli Zhang ^{1,2}, Jinming Zhang ², Yushan Ni ^{1,*}, Can Wang ², Kun Jiang ² and Xuedi Ren ²

¹ Department of Aeronautics and Astronautics, Fudan University, Shanghai 200433, China; zhangzl@simt.com.cn

² Shanghai Institute of Measurement and Testing Technology, Shanghai 201203, China; zhangjm@simt.com.cn (J.Z.); wangc@simt.com.cn (C.W.); Jiangk@simt.com.cn (K.J.); renxd@simt.com.cn (X.R.)

* Correspondence: niyushan@fudan.edu.cn

[†] Presented at the 1st International Electronic Conference on Crystals, 21–31 May 2018. Available online: https://sciforum.net/conference/IECC_2018.

Published: 21 May 2018

Abstract: Microscopic properties of nanocrystal Aluminum thin film have been simulated using the quasicontinuum method in order to study the surface defect influence in nanoindentation. Various distances between the surface defect and indenter have been taken into account. The results show that as the distance between the pit and indenter increases, the nanohardness increases in a wave pattern associated with a cycle of three atoms, which is closely related to the crystal structure of periodic atoms arrangement on {111} atomic close-packed planes of face-centered cubic metal; when the adjacent distance between the pit and indenter is more than 16 atomic spacing, there is almost no effect on nanohardness. In addition, the theoretical formula for the necessary load for the elastic-to-plastic transition of Al film has been modified with the initial surface defect size, which may contribute to the investigation of material properties with surface defects.

Keywords: nanoindentation; quasicontinuum method; surface defect; multiscale simulation

1. Introduction

Nanoindentation [1], which is relatively simple and effective, has already been a standard technique for evaluating the mechanical properties of thin films, widely used in many research fields [2–7]. Recently, a number of relevant scientists have focused on thin films with defects through simulations and experiments [8–11]. Wenshan Yu and Shengping Shen observed the strong effects of the geometry of the nanocavity as a kind of defect in the film during nanoindentation [12]. So far, surface roughness has become a major concern, which can be treated by the assembly of pits and steps [13,14]. Furthermore, the pitted surface can usually be seen in polycrystalline, microchips, MEMS (micro-electro-mechanical systems), and nanoindentation technology, as one typical kind of defect. Consequently, it is necessary and significant to make an observation on the nature of the pitted surface in nanoindentation. Ni yushan et al. [15] have already studied the nanoindentation of Al thin film compared with a surface defect situation and defect-free situation by multi-scale simulation, and Zhang Zhongli et al. [16] have identified the delay effect of dislocation nucleation with a surface pit in nanoindentation. But the distance effect between the pit and indenter on elastic-plastic transition has not been taken into account, which is especially important for the thin film performance in nanoindentation and microchips. Our aim is to assess the distance effect of the pitted surface on nanohardness by the quasicontinuum (QC) method [17], which is an effective way of investigating a large-scale simulation.

In the present article, fifteen distances of an adjacent boundary between the surface pit and indenter have been simulated by the QC method to investigate the distance effect of the pitted surface on nanohardness in nanoindentation. Compared with the nanoindentation on the defect-free surface, the distance effect of the pitted surface on elastic-plastic transition has been well explored and the theoretical formula of the critical load for dislocation emission has been modified with the initial surface pit.

2. Methodology

The Quasicontinuum (QC) method [18] is an effective mixed continuum and atomistic approach for simulating the mechanical response, especially in large-scale materials. The Ercolessi-Adams potential, which is one of the EAM potentials [19–22], is applied in this simulation to describe the atomistic behavior. Figure 1 shows the nanoindentation model used in the simulation and the corresponding schematic of local and non-local representative atoms with an initial surface pit. The relevant material parameters of the model are as follows: the crystallographic lattice constant a_1 is 0.4032 nm; one atomic spacing in the $[\bar{1}10]$ direction (h_0) is 0.1426 nm; Burgers vector \vec{b} is 0.285 nm; shear modulus μ is 33.14 GPa; Poisson ν is 0.319; and (111) surface energy γ_{111} is 0.869 J/m², which is comparable to the experimental values of 1.14–1.20 J/m². The elastic modules predicted by this potential are $C_{11} = 117.74$ GPa, $C_{12} = 62.06$ GPa, and $C_{44} = 36.67$ GPa. The experimental values extrapolated to $T = 0$ K are $C_{11} = 118.0$ GPa, $C_{12} = 62.4$ GPa, and $C_{44} = 32.5$ GPa [19]. The rectangular indenter is set rigid with its width of 9.32 Å (four times the lattice constant of Al). It is necessary to note that the indenter size is chosen based on the simulation example in the QC method manual and does not affect the behavior in the vicinity of the indenter. The indenter shape is chosen to be rectangular in this simulation because the boundary of the energy field and the distance between the pit and the indenter remain unchanged when driven down into the $(\bar{1}10)$ surface, which is necessary to investigate the distance influence of the pit. The width D and depth H of the surface pit are 0.688 nm and 0.730 nm, respectively. We take such size values because they are moderate and proper for investigating the distance effect of a pitted surface. When the pit is too small, the influence of the pit on the nanohardness is not obvious; when the pit is too large, the variation of nanohardness does not display much sensitivity to the distance between the pit and the indenter. In the out-of-plane direction, the thickness of this model is equal to the minimal repeat distance with the periodic boundary condition applied. The distance of the adjacent boundary between the pit and indenter is shown as d in Figure 1. Fifteen different distances of adjacent boundary d have been simulated in this paper, which are $1d_0$, $2d_0$, $3d_0$, $4d_0$, $5d_0$, $6d_0$, $7d_0$, $8d_0$, $9d_0$, $10d_0$, $11d_0$, $12d_0$, $13d_0$, $17d_0$, and $21d_0$, respectively, where d_0 is 0.2328 nm (one atomic lattice spacing in the $[111]$ direction). These distance situations are selected in order to make a more comprehensive investigation.

The thin Al film in this simulation is 0.1 μm in height and 0.2 μm in width, as shown in Figure 1, which is very large in normal atomistic modeling standards, with almost 1.3 million atoms or about 4 million degrees of freedom. By contrast, the multiscale simulation conducted by the QC method uses continuum assumptions for reducing the degrees of freedom and computational demand without losing the atomistic details required. At most, only 4000 atoms or 12,000 degrees of freedom are treated and such a simulation can be run on a personal computer in a few days.

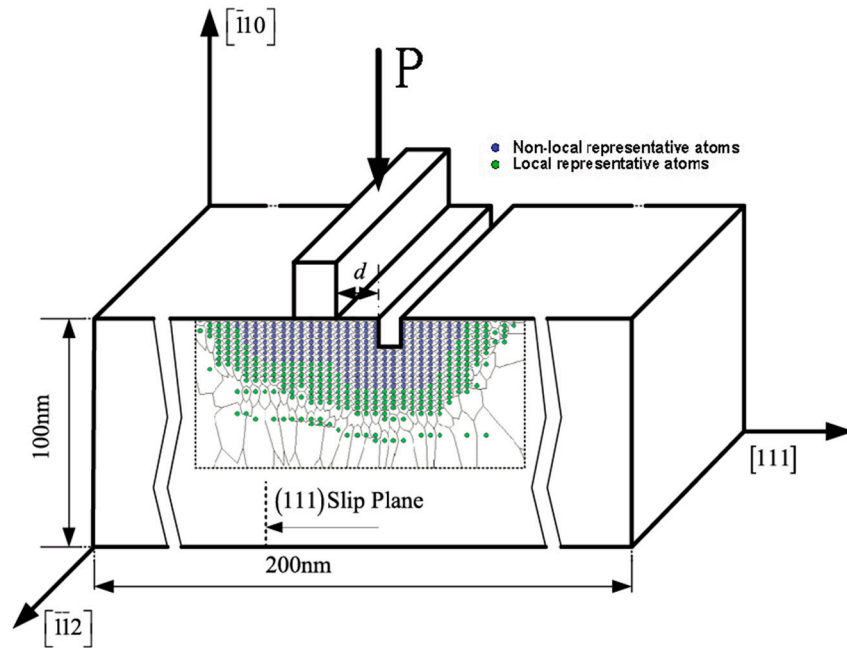


Figure 1. The schematic illustration of the nanoindentation model with a concave defect, where the unusual shapes in the local region are not finite elements, and they are just the schematic of its specific region that one corresponding representative atom belongs to.

3. Results and Discussion

3.1. Nanohardness in the Case of No Surface Defect

To make a comparison, a study of nanoindentation on the defect-free surface is carried out. The load-displacement curve showing the basic information obtained from nanoindentation simulations on the defect-free surface is presented in Figure 2, where the load is expressed by length units of the indenter in the out-of-plane direction with its unit N/m. It can be seen from Figure 2 that the load curve gradually increases during the initial loading process (OA), which indicates the elastic stage of thin film. The load increases to a maximum value of 15.14 N/m when the load step reaches 0.48 nm at point A. Then, the load experiences an abrupt drop, at which point it continually decreases to a minimum value of 7.67 N/m at point B.

To probe the potential mechanism of such an abrupt decline of load (AB segment in Figure 2), the atoms snapshot and corresponding out-of-plane displacements experienced by the atoms are investigated. Figure 3 shows the structure of atoms at the steps of 0.48 nm and 0.50 nm, which are corresponding point A and point B in Figure 2, respectively.

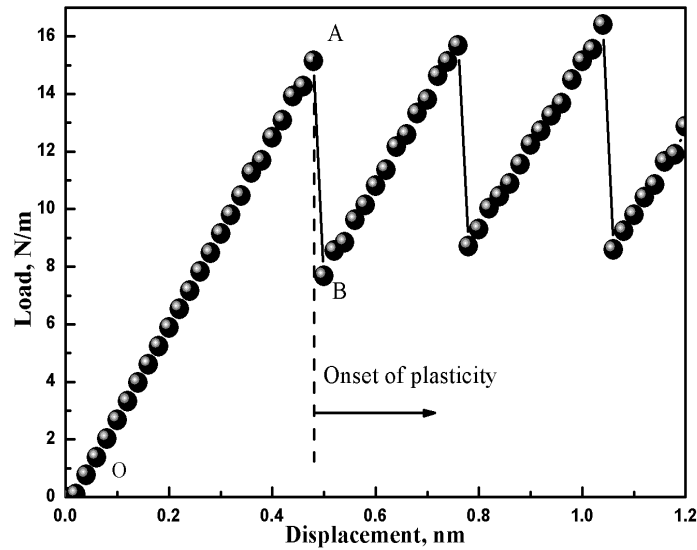


Figure 2. Load-displacement curves for nanoindentation on an Al film without a surface pit.

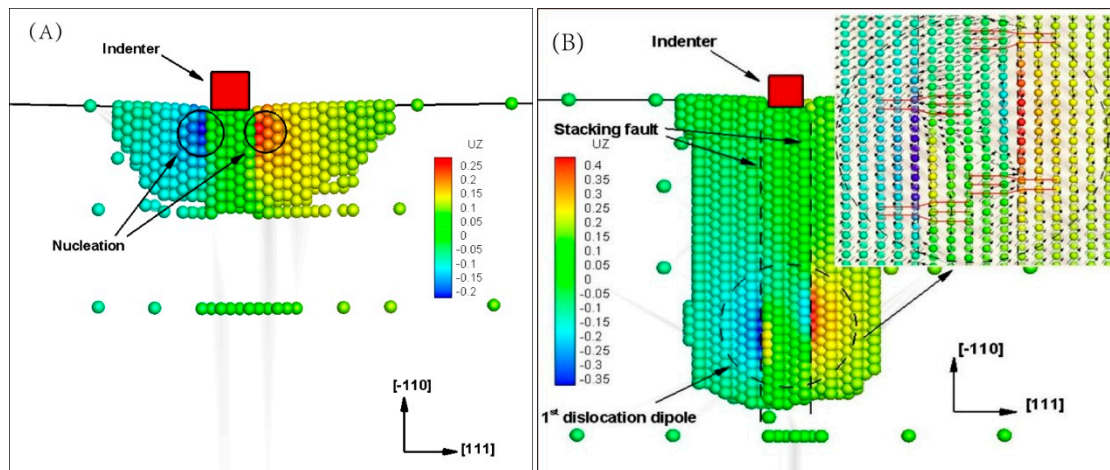


Figure 3. Snapshot of atoms under an indenter and corresponding out-of-plane displacement plot, where UZ is atom displacement at out-of-plane: (A) point A in Figure 3 (dislocation nucleation); (B) point B in Figure 3 (dislocation emission).

The conclusion can be drawn from Figure 3 that the load reaches the critical value for dislocation emission at point A, which indicates the beginning of the plastic deformation stage. Then, two Shockley partial dislocations are emitted at point B. The hardness is given by the equation [23]: $H = \frac{P_{max}}{A}$, where P_{max} is the maximum load and A is the indentation area, and the nanohardness of the Al thin film is 16.24 GPa with no surface defect.

In this simulation, the indenter width is 0.932 nm and the yield load is about 15.14 N/m, which is smaller than the value of 24.7 N/m obtained in the research of Tadmor and Miller [24] with a defect-free surface, where the indentation size is 2.5 nm. It is reasonable that a reduced width of the indenter will cause a significant decrease in the yield load, which is consistent with a published observation [25].

3.2. Nanohardness with Various Distances between Surface Defect and Indenter

Figure 4 shows each nanohardness value in the case of nanoindentation on the thin film surface with and without a surface pit. It indicates that the nanohardness of the pitted surface is reduced, compared to the one with no surface defect. This is reasonable because the atomic structure of the

thin film has been destroyed by the surface pit. Further, when the distance of the adjacent boundary between the pit and indenter d respectively equals $1d_0$, $2d_0$, $3d_0$, $4d_0$, $5d_0$, $6d_0$, $7d_0$, $8d_0$, $9d_0$, $10d_0$, $11d_0$, $12d_0$, $13d_0$, $17d_0$, or $21d_0$, the nanohardness curve rises up in a wave pattern and finally tends towards the nanohardness value of no surface defect.

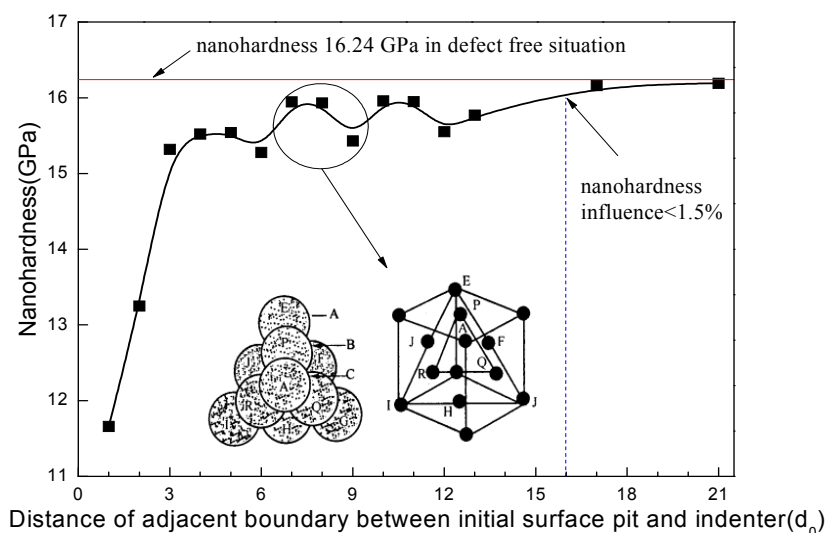


Figure 4. Nanohardness vs. distance of adjacent boundary between the pit and indenter.

Through a further investigation, the change law of nanohardness is discovered and such a wave pattern is associated with a cycle of three atoms (donated by circle in Figure 4), which is closely related to the crystal structure of the arrangement of periodic atoms. The scientific definition of a “crystal” is based on the microscopic arrangement of atoms inside it, called the crystal structure, where the atoms form a periodic arrangement [26]. Moreover, different stacking patterns of atoms have different gaps between adjacent atoms, which has a great influence on the performance of metal. In this simulation, such a periodic arrangement of atoms is “ABCABC” on {111} atomic close-packed planes of face-centered cubic metal (as shown in Figure 4 in the illustration). According to this simulation, when the simulation distance d increases each of the three atoms’ spacing in the [111] direction, one cycle of atoms arrangement in the “ABCABC” pattern is finished. That is why the nanohardness curve increases in a wave pattern associated with a cycle of three atoms.

In order to figure out the spatial extent of the influence of the surface pit on nanohardness, a further discussion is carried out. As Figure 4 shows, when the distance between the pit and indenter increases, the influence of nanohardness compared with the nanohardness of no surface defect (16.24 GPa) is running low. If the influence of nanohardness is smaller than 1.5%, it can be considered that the surface pit almost does not affect the nanohardness. According to this simulation, when the distance (d) is more than 16 atomic spacing, there is almost no effect on nanohardness (as shown in Figure 4). It can be predicted that different materials have different critical values, which has a significant meaning for the size design of thin layers in nanoindentation or microchips with the hardness guarantee.

However, the first three atoms, respectively $d = 1d_0$, $d = 2d_0$, and $d = 3d_0$ distance, do not match the wave pattern. To explain such a special phenomenon, the atomic structure and corresponding strain distribution of Al crystal are probed.

Figure 5 shows von Mises strain distribution of notch propagation and a comparison of strain before and after the notch when the distance d respectively equals $1d_0$, $2d_0$ and $3d_0$. It shows that when the distance d equals $1d_0$ and $2d_0$, there appears a notch phenomenon at the left side of surface pit, which directly induces serious damage to the structure of materials and great strain concentration (as shown in Figure 5A–D). When the distance d equals $3d_0$, there is no notch (as shown in Figure 5E,F). Consequently, when the distance d equals $1d_0$ and $2d_0$, the nanohardness is

greatly reduced. That is to say that the first three atoms in nanohardness curve as shown in Figure 4 will not match the wave pattern associated with a cycle of three atoms.

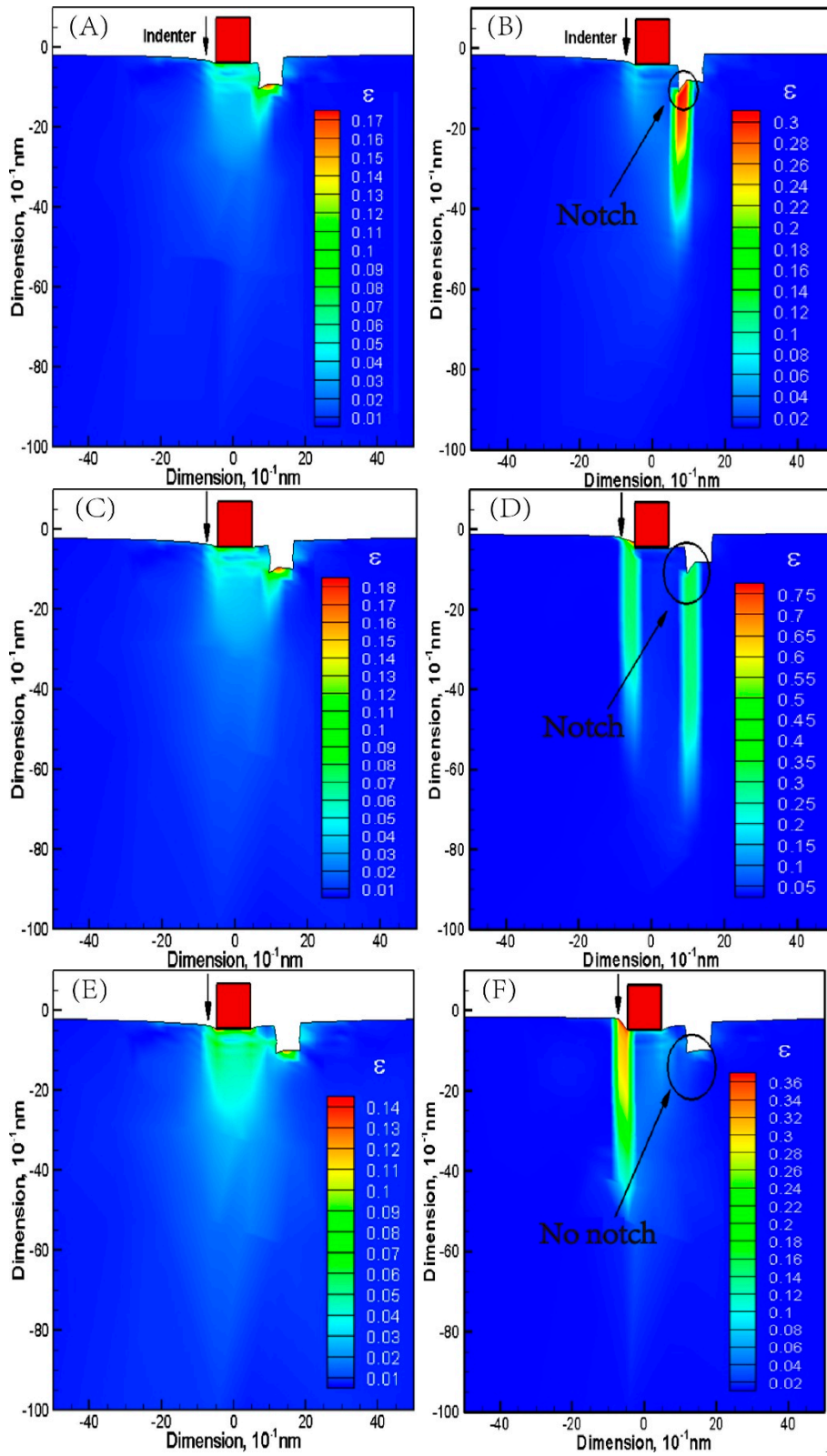


Figure 5. Von Mises strain distribution of notch propagation: (A) $d = 1d_0$ at the load step of the indenter 0.38 nm; (B) $d = 1d_0$ at the load step of the indenter 0.4 nm; (C) $d = 2d_0$ at the load step of the indenter 0.44 nm; (D) $d = 2d_0$ at the load step of the indenter 0.46 nm; (E) $d = 3d_0$ at the load step of the indenter 0.46 nm; (F) $d = 3d_0$ at the load step of the indenter 0.48 nm.

3.3. Formula Modification of Necessary Load for Elastic-to-Plastic Transition

It is known that the influence of the surface pit on nanohardness is actually the influence of dislocation nucleation and emission, which are affected by the surface pit. In order to conduct a further study on the nanohardness calculation in the case of a pitted surface, the calculation formula of the necessary load for elastic-to-plastic transition is discussed and modified based on the model with no surface defect.

According to the critical load for dislocation emission, which is applied by Tadmor [24], the calculation formula of the critical load for dislocation emission is displayed as follows:

$$P_{cr} = \frac{\mu b}{4\pi(1-\nu)} \ln \frac{32h(h+2a)a^2}{b^4} + 2\gamma_{111} + \frac{1}{2}kb \quad (1)$$

where P_{cr} is the critical load value at the onset of dislocation emission, k is the slope of the elastic stage in the load-displacement curve, h is the depth of the dislocation dipole when it is emitted, a is the half width of the indenter, and γ_{111} is the energy of the (111) surface of the Al crystal.

In order to make a more reasonable investigation, the data of simulation that $d = 1d_0$ and $d = 2d_0$ is not taken into account because of notching.

Table 1 shows the comparison of the critical load between the QC method and dislocation theory, where “QC data” means the data of the critical load in this simulation, and “theory load” means the data of the critical load using Equation (1). It shows that in the case of every distance (d) simulation, the difference value between the QC method and dislocation theory changes frequently. According to the phenomenon discussed above, where the nanohardness is periodically changed in a circle of three atoms, the critical load for dislocation emission is also in such periodicity. Consequently, the correction term (set as Δ) can be separated into two parts:

$$\Delta = A(d) + B \cdot \text{Sin}(d) \quad (2)$$

where $A(d)$ is the correction part for the hardness decrease because of the surface pit and $B \cdot \text{Sin}(d)$ is just for the periodic change of atoms arrangement. It is well known that when the pit size (D, H as shown in Figure 1) is bigger, the value of the critical load of dislocation emission is smaller. So, it is

reasonable to apply $\frac{D}{a_1} \cdot \frac{H}{a_1}$ (dividing by the crystallographic lattice constant can significantly

make it dimensionless, which has already been demonstrated as reasonable in a published article [27]) to express the size influence of the surface pit. When the surface pit is infinitely far away from the indenter, the influence on nanohardness can be ignored. Additionally, if the pit size increases, the correction term changes more slowly with the distance variation. So, it is reasonable to apply

$\ln(1 + (\frac{d_0}{d})^{\frac{d_0 \cdot h_0}{D \cdot H}})$ to express the distance effect of the surface pit. Furthermore, the affect of the

surface pit is closely related to the material property, such as the Burgers vector \vec{b} , shear modulus μ , and Poisson ν . According to Equation (1), it is reasonable to apply $\frac{\mu b}{4\pi(1-\nu)}$ to express the

influence of material property. In addition, on {111} atomic close-packed planes of face-centered cubic metal, the periodic atoms arrangement is “ABCABC”. So, the periodicity is three atoms. That is

to say, it is reasonable to apply $\text{Sin}(\frac{2\pi}{3d_0} \cdot d + \varphi)$ to express the periodicity of atoms arrangement.

Considering that the unit of correction term (Δ) is N/m, and according to the discussion above, the correction term can be defined as follows:

$$\Delta = \alpha \cdot \frac{\mu b D H}{4\pi(1-\nu)a_1^2} \ln(1 + (\frac{d_0}{d})^{\frac{d_0 \cdot h_0}{D \cdot H}}) + \beta \cdot \frac{\mu b}{4\pi(1-\nu)} \cdot \text{Sin}(\frac{2\pi}{3d_0} \cdot d + \varphi) \quad (3)$$

where α , β , φ are three constants that need to be optimized. According to the simulation data in Table 1, these three constants α , β , and φ are approximately $\frac{3}{2}$, $\frac{2}{15}$, and $-\frac{\pi}{3}$, respectively. So, the theoretical formula for the necessary load of the first dislocation emission of Al film has been modified with an initial surface pit as follows:

$$P_{cr}^* = \frac{\mu b}{4\pi(1-\nu)} \ln \frac{32h(h+2a)a^2}{b^4} + 2\gamma_{111} + \frac{1}{2}kb - \frac{3\mu bDH}{8\pi(1-\nu)a_1^2} \ln\left(1 + \left(\frac{d_0}{d}\right)^{\frac{d_0}{D} \frac{h_0}{H}}\right) - \frac{\mu b}{30\pi(1-\nu)} \cdot \text{Sin}\left(\frac{2\pi}{3d_0} \cdot d - \frac{\pi}{3}\right) \tag{4}$$

Figure 6 shows the comparison of the necessary load for elastic-to-plastic transition of Al thin film with various distances between the pit and the indenter calculated by the theoretical formula before and after modification. Though there is no parameter d in the unmodified dislocation theory (Equation (1)), the curves with blocks are calculated by each depth h corresponding to each distance case of the surface pit and indenter in this simulation. It shows that the simulation QC data are closer to the theoretical results which are calculated by Equation (4) after modification. That is to say, such modification to the theoretical formula is reasonable and efficient, and the pit size and the distance between the pit and indenter have both been taken into account.

This modified formula has performed well with regards to the decreasing trend of nanohardness as the distance between the pit and indenter increases. Such a trend greatly agrees with the experimental results of the surface step with various distances [14]. Moreover, this modification may contribute to the investigation of the material properties influenced by the surface defects, particularly in nanoindentation, MEMS, and microchips.

Table 1. The comparison of critical load between the QC method and dislocation theory.

Distance (d ₀)	QC Data (N/m)	Theory Load (N/m)	Data Difference (N/m)
3	14.28	18.02	3.75
4	14.46	17.29	2.83
5	14.48	17.88	3.39
6	14.24	17.41	3.15
7	14.86	17.96	3.14
8	14.85	17.65	2.83
9	14.38	17.92	3.07
10	14.87	17.87	3.49
11	14.86	18.03	3.16
12	14.49	17.56	2.70
13	14.70	17.99	3.50
17	15.06	18.04	3.34
21	15.09	18.17	3.11

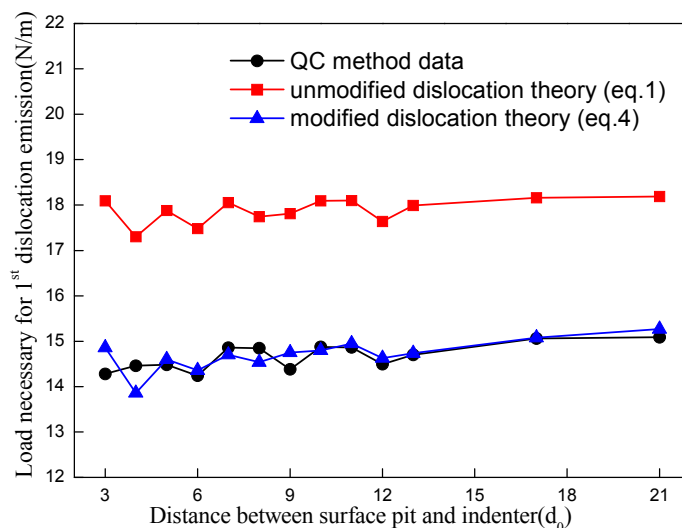


Figure 6. The comparison of the necessary load for elastic-to-plastic transition of Al thin film with various distances between the pit and the indenter calculated by the theoretical formula before and after modification.

4. Conclusions

In this paper, the QC method is employed to investigate the distance effect of the pitted surface on elastic-plastic transition. Compared with the nanoindentation on a defect-free surface, fifteen various distances of the adjacent boundary between the pit and indenter are taken into account. The following conclusions can be drawn:

- i. The pitted surface plays a great role in the emission of dislocation that causes a significant reduction in nanohardness, compared with the defect-free situation.
- ii. As the distance between the pit and indenter increases, the nanohardness increases in a wave pattern associated with a cycle of three atoms, which is closely related to periodic atoms arrangement on {111} atomic close-packed planes of face-centered cubic metal; when the adjacent distance between the pit and indenter is more than 16 atomic spacing, there is almost no effect on nanohardness, suggesting that each material has such a critical value.
- iii. The theoretical formula for the necessary load of the elastic-plastic transition of Al film has been reasonably and efficiently modified with an initial surface pit. This modified formula has performed well with regards to the decreasing trend of nanohardness as the distance between the pit and indenter increases, and such a trend greatly agrees with the experimental results of the surface step with various distances. Such modification may contribute to the investigation of material properties with surface defects, particularly in nanoindentation and microchips.

Acknowledgments: This work is supported by the National Natural Science Foundation of China (Grant No. 11572090). The authors would like to thank Professor Tadmor E. B. and Miller R. for their quasicontinuum code and suggestions during the multiscale simulations.

References

1. Oliver, W.C.; Pharr, G.M. An improved technique for determining hardness and elastic modulus using load and displacement sensing indentation experiments. *J. Mater. Res.* **1992**, *7*, 1564–1583.
2. Li, X.D.; Bhushan, B. A review of nanoindentation continuous stiffness measurement technique and its applications. *Mater. Charact.* **2002**, *48*, 11–36.
3. Bamber, M.J.; Cooke, K.E.; Mann, A.B.; Derby, B. Accurate determination of Young's modulus and Poisson's ratio of thin films by a combination of acoustic microscopy and nanoindentation. *Thin Solid Films* **2001**, *399*, 299–305.
4. Zhu, P.Z.; Hu, Y.Z.; Fang, F.Z.; Wang, H. Multiscale simulations of nanoindentation and nanoscratch of single crystal copper. *Appl. Surf. Sci.* **2012**, *258*, 4624–4631.

5. Chen, J.; Bull, S.J. Assessment of the toughness of thin coatings using nanoindentation under displacement control. *Thin Solid Films* **2006**, *494*, 1–7.
6. Sangwal, K.; Gorostiza, P.; Sanz, F. Atomic force microscopy study of nanoindentation creep on the (100) face of MgO single crystals. *Surf. Sci.* **2000**, *446*, 314–322.
7. Zhang, T.H.; Yang, Y.M. The application of nanohardness technology in the mechanical properties testing of surface engineering. *Chin. Mech. Eng.* **2002**, *24*, 85–88.
8. Mitchell, T.E. Dislocations and plasticity in single crystals of face centered cubic metals and alloys. *Prog. Appl. Mater. Res.* **1964**, *6*, 117–238.
9. Mitchell, J.W. *Growth and Perfection of Crystals*; Doremus, R.H., Roberts, B.W., Turnbull, D., Eds.; Wiley: New York, NY, USA, 1958; pp. 386–389.
10. Yang, B.; Vehoff, H. Dependence of nanohardness upon indentation size and grain size—A local examination of the interaction between dislocations and grain boundaries. *Acta Mater.* **2007**, *55*, 849–856.
11. Soifer, Y.M.; Verdyan, A.; Kazakevich, M.; Rabkin, E. Nanohardness of copper in the vicinity of grain boundaries. *Scr. Mater.* **2002**, *47*, 799–804.
12. Yu, W.S.; Shen, S.P. Multiscale analysis of the effects of nanocavity on nanoindentation. *Comp. Mat. Sci.* **2009**, *46*, 425–430.
13. Shan, D.; Yuan, L.; Guo, B. Multiscale simulation of surface step effects on nanoindentation. *Mat. Sci. Eng. A* **2005**, *412*, 264–270.
14. Keily, J.D.; Hwang, R.Q.; Houston, J.E. Effect of surface steps on the plastic threshold in nanoindentation. *Phys. Rev. Lett.* **1998**, *81*, 4424–4427.
15. Li, J.W.; Ni, Y.S.; Lin, Y.H.; Luo, C. Multiscale simulation of nanoindentation on Al thin film. *Acta Metall. Sin.* **2009**, *45*, 129–136.
16. Zhang, Z.L.; Ni, Y.S. Multiscale analysis of delay effect of dislocation nucleation with surface pit defect in nanoindentation. *Comp. Mat. Sci.* **2012**, *62*, 203–209.
17. Qin, Z.D.; Wang, H.T.; Ni, Y.S. Multiscale simulations of FCC Al nanoindentation. *Chin. Q. Mech.* **2007**, *1*, 46–53.
18. Tadmor, E.B. The Quasicontinuum Method. PhD Thesis, Brown University, Providence, RI, USA, 1996.
19. Ercolessi, F.; Adams, J.B. Interatomic potentials from first-principles calculations: The force-matching method. *Europhys. Lett.* **1994**, *26*, 583–588.
20. Tadmor, E.B.; Ortiz, M.; Phillips, R. Quasicontinuum analysis of defects in solids. *Philos. Mag. A* **1996**, *73*, 1529–1563.
21. Tadmor, E.B.; Phillips, R.; Ortiz, M. Mixed atomistic and continuum models of deformation in solids. *Langmuir* **1996**, *12*, 4529–4534.
22. Shenoy, V.B.; Miller, R.; Tadmor, E.B.; Rodney, D.; Phillips, R.; Ortiz, M. An adaptive finite element approach to atomic-scale mechanics—The quasicontinuum method. *Mech. Phys. Solids.* **1999**, *47*, 611–642.
23. Nanoindentation. Available online: <https://en.wikipedia.org/wiki/Nanoindentation> (accessed on 2 May 2018).
24. Tadmor, E.B.; Miller, R.; Phillips, R. Nanoindentation and incipient plasticity. *J. Mater. Res.* **1999**, *14*, 2233–2250.
25. Jiang, W.G.; Li, J.W.; Su, J.J.; Tang, J.L. Quasicontinuum analysis of indenter size effect in nanoindentation tests. *Chin. J. Solid Mech.* **2007**, *4*, 375–379.
26. Crystal Structure. Available online: https://en.wikipedia.org/wiki/Crystal_structure (accessed on 20 June 2018).
27. Abu Al-Rub, R.K.; Voyiadjis, G.Z. A physically based gradient plasticity theory. *Int. J. Plast.* **2006**, *22*, 654–684.

